Crossed-beam chemiluminescent studies of alkaline earth atoms with ClO_2

F. Engelke,* R. K. Sander,† and R. N. Zare

Department of Chemistry, Columbia University, New York, New York 10027
(Received 18 March 1976)

Chemiluminescence resulting from the reaction $M+ClO_2$, M = Mg, Ca, Sr, or Ba, has been observed in crossed molecular beams. Two special features are found: (1) selective formation of MO* in the $A'\,^1\Pi$ state in preference to the isoenergetic $A\,^1\Sigma^+$ state; and (2) the formation of MCl* in various electronic states. Although the MCl* product results from attack of the central Cl atom in ClO_2, its cross section is comparable to that of MO*. The cross section for chemiluminescence is a small fraction of the total reaction cross section, which is larger than gas kinetic. From the chemiluminescent spectra the relative electronic, vibrational, and rotational population distributions are derived and the following lower bounds are placed on the MO dissociation energies: $D_0^0(CaO) \geq 109.7 \pm 3.5$ kcal/mole; $D_0^0(SrO) \geq 107.7 \pm 3.5$ kcal/mole; and $D_0^0(BaO) \geq 133.6 \pm 3.5$ kcal/mole. The reaction dynamics are discussed in terms of an electron transfer from M to the half-filled antibonding orbital of ClO_2.

I. INTRODUCTION

The study of chemiluminescent processes in gases has a long and colorful history,[1] but only with the advent of beam studies[2] under single-collision conditions has it become a useful tool for understanding the detailed dynamics of highly exothermic chemical reactions. From the chemiluminescent spectrum it is possible to identify the emitting species and to determine the population distribution of the internal states, electronic, vibrational, and rotational. We present here an investigation of the chemiluminescent emission resulting from the reaction of the alkaline earth metals, M = Mg, Ca, Sr, and Ba, with chlorine dioxide, ClO_2.

Previous studies in our laboratory have employed O_3, N_2O, NO_2, and halogen molecules as reactants with a beam–gas arrangement.[3–9] This work is the first usage of ClO_2 and uses true crossed molecular beams.[10] We have deduced the existence of three different products, MCl*, MO*, and ions.[11] The MCl product is particularly remarkable because its formation in the reaction M + OClO involves a rearrangement in which two "old" Cl–O bonds are broken and two "new" bonds, MCl and O_2, are formed. Chemical attack of the central atom of a triatomic in a single collisional encounter appears to be almost unprecedented.[12] The electronic state of the MO* product is also unexpected *a priori* since only the $A'\,^1\Pi$ state is produced in the reaction, although the much better known $A\,^1\Sigma^+$ state lies at the same energy. Nonetheless, we shall show that both these features may be rationalized using an electron-jump model and simple molecular orbital arguments.

Following a discussion of the experimental procedure, we present the chemiluminescent spectra from which are derived electronic, vibrational, and rotational population distributions, as well as lower bounds to dissociation energies. Although chemiluminescence studies are blind to the formation of ground state products, we have obtained the total reactive cross section and the photon yield for each metal. From this information the fraction of ground state products is inferred to be nearly unity under these single-collision conditions.

II. EXPERIMENTAL

A beam apparatus, called LABSTAR, has been described previously.[3] We note here the modifications made to study the reactions of Group IIa metal atoms with chlorine dioxide (see Fig. 1).

A vertical metal beam crosses a poorly collimated horizontal beam of ClO_2. The metal vapor is produced in a resistance-heated, disposable, stainless steel oven. The temperature of the oven is chosen to give about 0.1–0.3 torr pressure of the metal vapor, which escapes through a 0.4 mm wide, 6 mm long rectangular slit. Under these conditions, there is a flux of 10^{18} atom/sec corresponding to 10^{15} atom/cm^2-sec in the reaction zone. Oven temperatures are monitored with either a chromel–alumel thermocouple or an optical pyrometer.

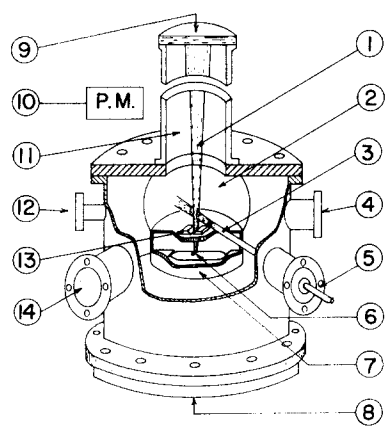

FIG. 1. Cut-away diagram of the experimental apparatus showing (1) the metal atom beam; (2) the 6 in. diffusion pump elbow; (3) the gas inlet tube, terminating in a multichannel array; (4) an observation port; (5) the gas inlet flange; (6) the metal atom oven; (7) the oven chamber; (8) the diffusion pump flange for the oven chamber; (9) the liquid-nitrogen-cooled flange used as a beam stop; (10) the photomultiplier which could be moved vertically to measure total cross sections; (11) a 0.5 m long glass tube; (12) port for ionization gauge; (13) metal beam collimating slits; and (14) the spectrometer viewing port.

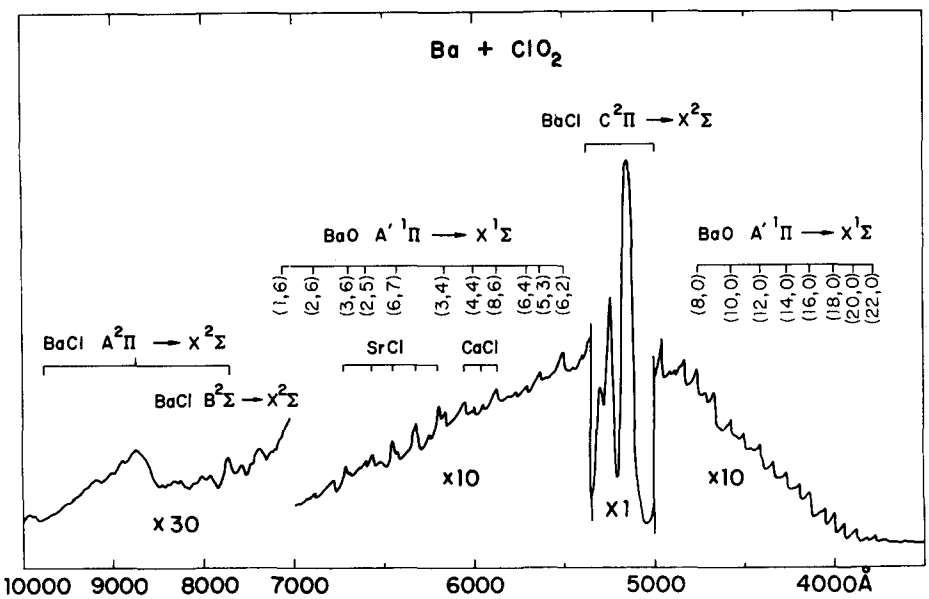

FIG. 2. The chemiluminescence spectrum from Ba + ClO_2, showing emission from the BaO A' state and BaCl A, B, and C states. Note that the wavelength scale is compressed for the BaCl A and B states and the intensity scale is expanded as marked.

The barium and strontium metals are obtained from Atomergic Chemical Co. with a stated purity of better than 99%. The main contaminant is calcium, which unfortunately contributed to some of the observed chemiluminescence. The calcium and magnesium metals are obtained from Fisher Scientific Co. (standard purity). All metals are used without further purification.

A separately pumped vacuum chamber contains the ClO_2 beam source, which is a multichannel stainless steel capillary array. The ClO_2 pressure behind the capillary array is approximately 1 torr. Although most single-collision chemiluminescence studies are done with a beam–gas configuration, the present experiment is operated as true crossed beams. When both beams are on, the pressure in the scattering chamber is typically 1×10^{-5} torr, as measured by a vacuum ionization gauge located 15 cm from the reaction zone. To avoid attack of the forepump by ClO_2, a demountable liquid-nitrogen-cooled trap is inserted in the foreline.

The ClO_2 is prepared according to Bray's method[13] utilizing potassium chlorate and moist oxalic acid. Chlorine dioxide is known to be an explosive material. However, there were no detonations when the proper precautions were followed, namely, if the ClO_2 is stored at $-78\,^{\circ}C$ (dry ice), at which temperature the gas pressure is about 1 torr. In addition, the ClO_2 must never be exposed suddenly to atmospheric pressure.

The chemical preparation of ClO_2 is carried out in a fume hood. All connections are lubricated with halocarbon grease. Reaction products are collected at $-196\,^{\circ}C$ (liquid nitrogen) and the chlorine dioxide is distilled into a 1 l bulb at $-78\,^{\circ}C$. The purity of the sample was checked by passing the gas through an HgI_2 trap.[14] Possible Cl_2, Cl_2O, and Cl_nO_m ($n \geq 2$) contaminants react with the red mercuric iodide to form colorless $HgCl_2$. No detectable change in color of the HgI_2 trap occurred.

The chemiluminescent spectra are taken as follows: The metal beam collimated by a 1.2 mm×10 mm slit crosses the roughly collimated ClO_2 beam in the reaction chamber (see Fig. 1). The chemiluminescence is observed by eye to originate primarily from the volume intersected by the two crossed beams. A 1-m f 5.6 Interactive Technology scanning spectrometer views the chemiluminescence through a quartz window at right angles to the metal beam. A quartz lens focuses the emission onto the entrance slit; a cooled Centronic S-20 extended red photomultiplier is attached to the exit slit. The solid angle subtended by the detection optics is 4×10^{-3} sr. The output of the photomultiplier is amplified by a Keithley model 417 picoammeter, which drives a stripchart recorder.

To check the stability of the beams, in some early experiments a second photomultiplier with filters was installed at another observation port in the scattering chamber. The emission spectra were obtained from the ratio of the outputs of the spectrometer and this detector. However, the beams were found to be sufficiently stable so that it was unnecessary to continue this ratio recording in subsequent experiments.

III. RESULTS

A. Spectral appearance

The chemiluminescence spectra for the reactions Ba + ClO_2, Sr + ClO_2, Ca + ClO_2, and Mg + ClO_2 are shown in Figs. 2–5, respectively. The emission extends over the entire visible spectrum for the first three reactions and is entirely in the ultraviolet for Mg. The spectra shown are uncorrected for the wavelength response of the detector, but the measured response function[7] is shown as a dashed line in Fig. 5. These spectra were measured with 10 Å resolution; individual bands and sequences were examined at 1 Å resolution in order to ensure correct identification of the bandheads and the nature of the electronic states. The MO A'–X band assignments are based on the work of Field[15] as confirmed and/or revised for BaO by Hsu *et al.*[16] and Wyss and Broida[17]; for SrO by Capelle, Broida, and Field[18]; and

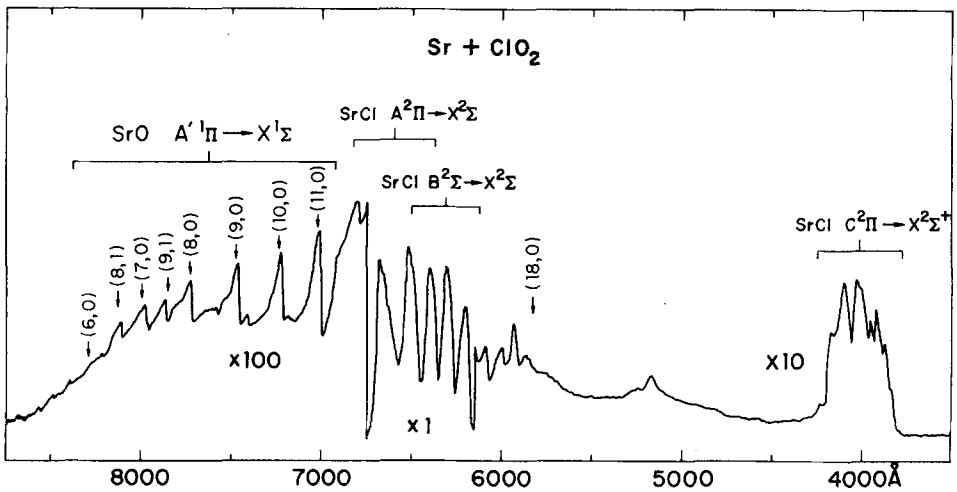

FIG. 3. The chemiluminescence spectum from $Sr + ClO_2$, showing emission from the SrO A' state and SrCl A, B, and C states. Note scale changes of the intensity vs wavelength for the A' state of SrO and the C state of SrCl.

for CaO by Field, Capelle, and Jones.[19]

In the BaO and SrO spectra, the low resolution and overlapping bands prevent us from excluding the possibility that no other bands may underlie the $A'-X$ emission. However, for BaO it is possible to conclude that the well known BaO $A-X$ system, if it is present at all, is at least 10 times less intense than the BaO $A'-X$ system. For SrO, even more stringent bounds (1 : 50) may be set. In the CaO spectrum (Fig. 4), some $A-X$ bandheads can be identified. However, the ratio of $A-X$ to $A'-X$ emission is about 1 : 100.

The MO $A'-X$ emission is more extensive than previously reported. The bandhead positions are readily determined because the overlapping MO $A-X$ bands are nearly absent. Table I lists the positions of the new MO $A'-X$ bandheads. The observed positions agree fairly well with those predicted by Field[15]; thus, no attempt was made to revise his vibrational constants.

Attention should be drawn to some features not observed which lend credence to our understanding of the reaction conditions. Atomic emission lines are entirely absent from these crossed-beam chemiluminescent spectra, unlike spectra often obtained with a beam–gas arrangement. Also absent is emission from electronic states too high in energy to be produced under single-collision conditions. Thus, in the $Mg + ClO_2$ reaction no MgO bands are observed, since the excited $A\,^1\Sigma$ state is not energetically allowed and the $A'\,^1\Pi-X\,^1\Sigma$ band system lies in the infrared.[18]

Other states that are produced in these reactions, although not observed directly by chemiluminescence, include ground state products and ionic products.[11] Metastable states with long radiative lifetimes such as the MO $^3\Pi$ states or the MCl $^2\Delta$ states may also be present, but are undetectable. However, the BaCl $A\,^2\Pi-X\,^2\Sigma^+$ and $B\,^2\Sigma^+-X\,^2\Sigma^+$ band systems are obtained by scanning the spectrometer to 11 000 Å, even though the S-20 photomultiplier response falls precipitously in this region. This observation implies that the BaCl A and B states are strongly populated by the $Ba + ClO_2$ reaction, either directly or by cascade. The cascade mechanism seems ruled out, however, since the $C-A$ and $C-B$ systems are known to be weak.[20]

B. Reaction order

The interpretation of these spectra in terms of single-collision reaction dynamics between a metal atom and a

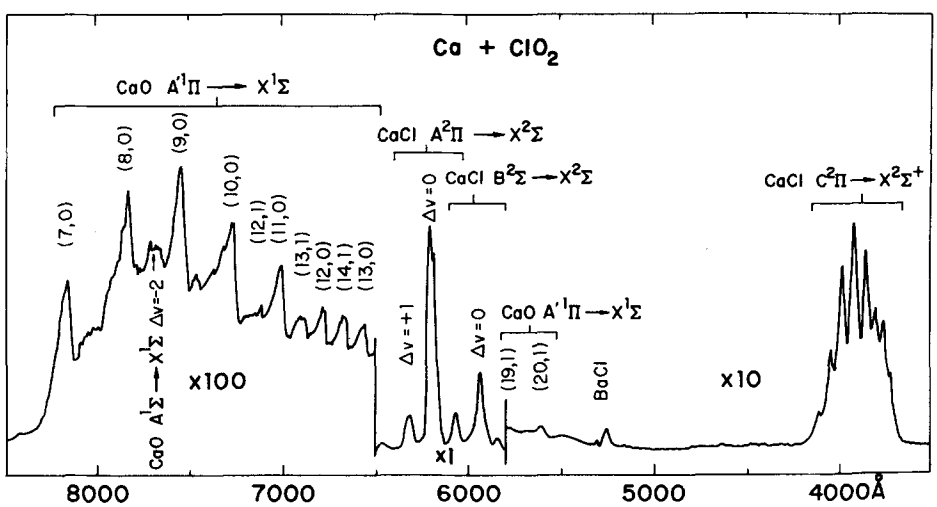

FIG. 4. The chemiluminescence spectrum from $Ca + ClO_2$, showing emission from the CaO A and A' states and the CaCl A, B, and C states. Note the scale changes in intensity, as marked.

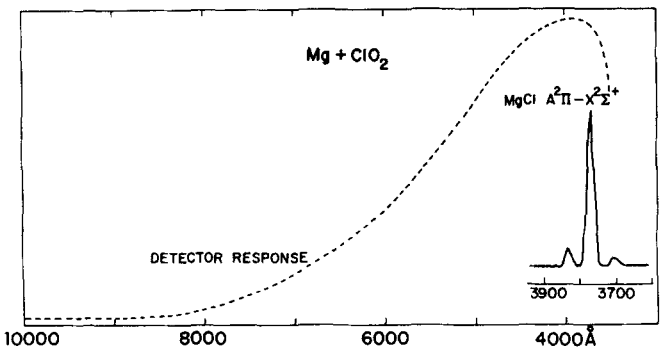

FIG. 5. The chemiluminescence spectrum from $Mg + ClO_2$, showing emission from the MgCl A state. The response as a function of wavelength is also indicated by a dashed curve and applies as well to Figs. 2–4. In Figs. 2–5, the intensity scale is linear in the photon emission rate.

chlorine dioxide molecule must have its validity proven. A powerful test of this point is made by measuring the intensity of chemiluminescent emission as a function of metal atom oven temperature. The results of this study are shown in Fig. 6. For each metal, the logarithm of the $M + ClO_2$ chemiluminescence intensity falls on a straight line plotted as a function of the reciprocal of the oven temperature. If the emission process involved two collisions with metal atoms, then the signal would be proportional to the square of the metal atom flux and hence the square of the pressure in the metal atom oven. This would cause the plots in Fig. 6 to depart from linearity. As is seen, the data provide convincing proof that one and only one metal species emanating from the oven participates in the reaction mechanism producing chemiluminescence.

TABLE I. New bandhead positions for the MO $A'\,^1\Pi - X\,^1\Sigma^+$ system.

	BaO		
(v', v'')	ν_{obs}	ν_{calc} [a]	ν_{calc} [b]
(6, 0)	20 173	20 164	20 173
(7, 0)	20 589	20 585	20 593
(8, 0)	21 003	21 002	21 009
(2, 6)	14 503	14 515	14 530
(3, 6)	14 943	14 949	14 963
(2, 5)	15 154	15 160	15 176
(6, 7)	15 576	15 590	15 600
(3, 5)	15 601	15 594	15 608
(2, 4)	15 810	15 810	15 825
(4, 5)	16 026	16 025	16 037
(3, 4)	16 247	16 244	16 257
(7, 6)	16 639	16 652	16 660
(4, 4)	16 667	16 675	16 687
(3, 3)	16 892	16 897	16 911
(8, 6)	17 050	17 069	17 076
(5, 4)	17 097	17 102	17 113
(4, 3)	17 325	17 328	17 340
(6, 4)	17 513	17 526	17 535
(5, 3)	17 762	17 755	17 766
	SrO		
(v', v'')	ν_{obs}	ν_{calc} [c]	
(5, 0)	12 077	12 049	
(6, 0)	12 516	12 492	
(9, 2)	12 535	12 718	
(10, 2)	12 960	12 940	
(9, 1)	13 170	13 365	
(11, 2)	13 383	13 365	
	CaO		
(v', v'')	ν_{obs}	ν_{calc} [d]	
(7, 0)	12 293	12 577	
(8, 0)	12 798	13 164	

[a]Reference 16.
[b]Reference 17.
[c]Reference 18.
[d]Reference 19.

The slopes of the straight lines in Fig. 6 provide further information on the nature of the metal species responsible for the chemiluminescent reactions. Assuming no activation energy for these exothermic reactions, the Clausius–Clapeyron equation predicts that the slopes of the lines should equal $\Delta H_{vap}(M)/R$, the atomic heat of vaporization of the metal divided by the gas constant. If the metal species is an electronically excited state of the atom, the slope is given by $[\Delta H_{vap} + \Delta E(M^*)]/R$, where $\Delta E(M^*)$ is the excitation energy of M^*. Similarly, if the metal species is a dimer M_2, then $\Delta H_{vap}(M)$ is replaced by $\Delta H_{vap}(M_2)$. Thus, it is reassuring to find that the slopes shown in Fig. 6 correspond to $\Delta H_{vap}(M)$ within 10% of the literature values.[21] This 10% variation is not surprising and may indicate a systematic error in measuring the true oven temperature, deviations from pure effusive beam conditions that change the effective volume of the reaction zone as a function of oven temperature, or the existence of a small activation energy. Hence, the $M + ClO_2$ chemiluminescent reactions are first order in the ground state metal atom M. A similar study of the chemiluminescence intensity as a function of the ClO_2 source pressure for a fixed metal atom flux shows that the chemiluminescence is first order in ClO_2. We conclude that a single reactive encounter between the metal atom M and ClO_2 produces the observed chemiluminescence.

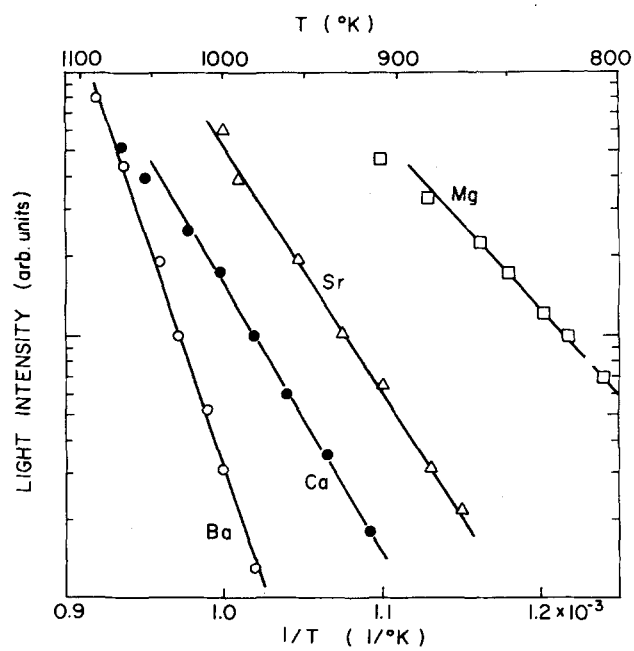

FIG. 6. The logarithm of the chemiluminescent intensity vs the reciprocal of the metal atom oven temperature. Straight lines indicate the linearity of the data points.

C. Dissociation energy

As shown in earlier papers,[2-4,8-10,22] chemiluminescence under single-collision conditions can be a useful means of determining lower limits on the dissociation energies of the product molecules. From energy conservation one obtains

$$\Delta E(\text{reaction}) + E_{\text{int}}(\text{reagents}) + E_{\text{trans}}(\text{reagents}) = E_{\text{int}}(\text{products}) + E_{\text{trans}}(\text{products}) , \quad (1)$$

where ΔE(reaction) is the reaction exoergicity, E_{int} is the internal energy, and E_{trans} is the relative translational energy.

The reaction energy for $M + ClO_2 \rightarrow MO + ClO$ is the energy difference between the new bonds formed and the old bonds broken, i.e.,

$$\Delta E(\text{reaction}) = D_0^0(\text{MO}) - D_0^0(\text{OCl–O}) . \quad (2)$$

There have been several determinations of the ClO_2 bond strength. Finkelnburg and Schumacher[23] obtain 66 ± 3 kcal/mole based on the spectroscopic observation of predissociation in ClO_2. Fisher[24] obtains 55 ± 2 kcal/mole based on ionization appearance potentials. Finally, thermochemical work[25] places D_0^0(OCl–O) at 57.6 ± 1.5 kcal/mole and agrees closely with Fisher's value. We adopt the value $D_0^0(\text{OCl–O}) = 58 \pm 3$ kcal/mole recommended by Darwent.[26]

The internal energy of the reagents is given primarily by the rotational energy of ClO_2, $\frac{3}{2}RT$, which equals 0.88 kcal/mole. To this, the slightly populated ClO_2 vibrational bending mode ($\nu_2 = 447$ cm^{-1}) adds 0.16 kcal/mole to the average reagent internal energy. Thus, $E_{\text{int}} = 1.0 \pm 0.2$ kcal/mole, where the error reflects uncertainty as to which of the reagent internal states contribute to the production of the highest vibrational level of the MO A' state. The internal energies of the product MO molecules are determined from the highest identified vibrational level in the A' state, shown in Figs. 2–4, and they are as follows: BaO, the (22, 0) band at 26 490 cm^{-1}; SrO, the (18, 0) band at 17 430 cm^{-1}; and CaO, the (20, 0) band at 18 300 cm^{-1}.

The reagent translational energy in the center of mass reference frame is calculated from the expression appropriate to perpendicular molecular beams

$$E_{\text{trans}} = \tfrac{1}{2}\mu(v_1^2 + v_2^2) , \quad (3)$$

where μ is the reduced mass of the collision partners and $v_i = (3RT_i/M_i)^{1/2}$ is the most probable velocity of molecular beam i with mass m_i and temperature T_i. The reagent translational energies are $E_{\text{trans}}(\text{Ba} + ClO_2) = 1.6 \pm 0.8$ kcal/mole; $E_{\text{trans}}(\text{Sr} + ClO_2) = 1.7 \pm 0.9$ kcal/mole; and $E_{\text{trans}}(\text{Ca} + ClO_2) = 2.1 \pm 1.0$ kcal/mole. The uncertainties represent estimates of the spread in the relative velocity distributions. The product translational energies are unknown, as is the internal energy of the ClO radical.

Substituting Eq. (2) into Eq. (1), using the above numerical values, and neglecting E_{trans}(prod) and E_{int}(ClO), we find the lower bounds:

$$D_0^0(\text{BaO}) \geq 133.6 \pm 3.5 \text{ kcal/mole} , \quad (4)$$

$$D_0^0(\text{SrO}) \geq 107.7 \pm 3.5 \text{ kcal/mole} , \quad (5)$$

$$D_0^0(\text{CaO}) \geq 109.7 \pm 3.5 \text{ kcal/mole} . \quad (6)$$

The uncertainty in each of the above three values is essentially the same, stemming primarily from the uncertainty in the ClO_2 bond strength.

The value for D_0^0(BaO) in Eq. (4) should be compared with the previous estimate of $D_0^0(\text{BaO}) \geq 133$ kcal/mole obtained from the chemiluminescent spectrum[3] of Ba + NO_2 and the determination of $D_0^0(\text{BaO}) = 133.5 \pm 1.3$ kcal/mole obtained from the laser-induced excitation spectrum[27] of BaO in the reaction Ba + CO_2. This excellent agreement may be taken as an indication that the value we use for D_0^0(OCl–O) is reasonable.

The values for D_0^0(SrO) and D_0^0(CaO) in Eqs. (5) and (6) deserve a more extended discussion since these lower limits raise questions about previous determinations. The value for SrO may be low since the highest energy bandhead might have been obscured by Ca impurity (see Fig. 3). A recent measurement by Batalli-Cosmovici and Michel[28] gives $D_0^0(\text{SrO}) = 112$ kcal/mole with an error estimate of $+3.4$ and -0.7 kcal/mole. Measurements of the alkaline earth monoxide dissociation energies have long been plagued by uncertainties in the low-lying electronic states and their dissociation products. Equilibrium measurements are affected through the calculated free energy function, which depends on the number and degeneracy of low-lying electronic states, while spectroscopic measurements are affected by the uncertainties in determining the dissociation products that correlate with the observed states. Consequently, measurements of the dissociation energy scatter more widely than would be expected from the individually quoted error limits. This situation is reflected in the recommended values by Gaydon[29] of $D_0^0(\text{CaO}) = 100 \pm 16$ kcal/mole and $D_0^0(\text{SrO}) = 97 \pm 14$ kcal/mole.

The review article by Brewer and Rosenblatt[30] discusses previous determinations. In general, spectroscopic extrapolations have not proved reliable, while flame photometry give high values and mass spectrometry low values. The latter have usually been given the most weight in recommending a bond dissociation energy.[31]

Two recent mass spectrometric determinations of the CaO and SrO bond energies are in excellent agreement with each other. Collin, Goldfinger, and Jeunehomme[32] studied the $M + SO \rightleftharpoons MO + S$ equilibrium; Drowart, Exsteen, and Verhagen[33] investigated the three reactions $MO + O \rightleftharpoons M + O_2$, $MO + MoO_2 \rightleftharpoons M + MoO_3$, and $MO + WO_2 \rightleftharpoons M + WO_3$. Two possible interpretations of the data are given by Brewer and Rosenblatt. Assuming a $^1\Sigma$ ground state and a low-lying $^3\Pi$ state yields a free energy function for MO such that the data of Colin *et al.* give $D_0^0(\text{CaO}) = 84.4 \pm 5$ kcal/mole and $D_0^0(\text{SrO}) = 92.3 \pm 6$ kcal/mole, while those of Drowart *et al.* give $D_0^0(\text{CaO}) = 83 \pm 5$ kcal/mole and $D_0^0(\text{SrO}) = 92.4 \pm 5$ kcal/mole. However, our present knowledge of the location of the CaO and SrO electronic states,[15] namely, that the ground state is a $^1\Sigma$ state and the closest low-lying state is a $^3\Pi$ state some 8225 cm^{-1} away for CaO and 9055 cm^{-1} for SrO, indicates that the alternative interpretation using

TABLE II. Electronic state distribution.

M	MO A	MO A'	MCl A	MCl B	MCl C
Ba	a	11	b	b	1
Sr	a	89	109	44	1
Ca	1	95	76	19	1

[a]Not identified as part of the chemiluminescent emission.
[b]No estimate is given here because the BaCl A–X and B–X band systems lie in the infrared where corrections for the detector response are large and uncertain.

a free energy function based on an isolated $^1\Sigma$ ground state is to be preferred. The data of Colin *et al.* then yield $D_0^0(CaO) = 93.7 \pm 6$ kcal/mole and $D_0^0(SrO) = 101.2 \pm 6$ kcal/mole while those of Drowart *et al.* give $D_0^0(CaO) = 95 \pm 5$ kcal/mole and $D_0^0(SrO) = 102.2 \pm 5$ kcal/mole. Nevertheless, our lower bounds of $D_0^0(CaO) \geq 109.7 \pm 3.5$ kcal/mole and $D_0^0(SrO) \geq 107.7 \pm 3.5$ kcal/mole strongly suggest that the mass spectrometric determinations are systematically low.

D. Internal state distributions

1. Electronic

By correcting the chemiluminescent spectra for the detector response and integrating the area under the assigned band systems, it is possible to obtain the relative populations of the excited electronic states of the products. In this procedure, the fractional contributions of overlapping spectral features are crudely estimated.

Table II presents the relative electronic populations of excited MCl* and MO*, normalized for each M to the MCl C state. These relative values are probably accurate to 20%, since they involve measurements in the region 3500–8000 Å. Emission of the CaO and SrO A' states beyond 8000 Å may contribute another 30% and 20%, respectively, to the total MO A' state emission with perhaps a 50% uncertainty in these numbers because of the calibration of the rapidly decreasing spectrometer and photomultiplier sensitivity.

Although MO* emission is seen in three reactions, only in the $Ca + ClO_2$ chemiluminescence is it possible to resolve a feature that can be definitely attributed to the well known MO $A\,^1\Sigma^+$ state. The relative amounts of CaO A and A' state emission are estimated from the total area under the CaO $A'\,^1\Pi$ emission and the area under the observed A–X $\Delta v = -2$ sequence (see Fig. 4). To obtain the total A state visible emission, the ratio of the sum of the $\Delta v = 0, -1, -2, -3, -4$, and -5 sequences to the $\Delta v = -2$ sequence was calculated, assuming equal populations in the energetically allowed $v' = 1$–8 levels of the A state, since these cannot be individually identified in the $\Delta v = -2$ sequence.

It can be seen from Table II that the production of MO* in the reaction $M + ClO_2$ is comparable to the production of MCl* (total A, B, and C states). Among the metal chloride excited states, the relative electronic populations follow the ordering $A > B > C$. However, these populations are only poorly described by an electronic temperature. It would appear that the relative electronic populations produced by the Ca and $Sr + ClO_2$ reactions are more similar to one another than either is to $Ba + ClO_2$.

In spite of the fact that there is sufficient energy to populate excited states above the C state for all MCl products, M = Ca, Sr, and Ba, we observe no emission from them. These excited states may lie above open ion channels.[11] We speculate that this may account for their absence.

2. Relative photon yield

The relative photon yield allows the intercomparison of the three metals in Table II, albeit with somewhat less precision than the normalized quantities given therein. For this purpose, the following procedure is carried out. A measured mixture of Ba, Sr, and Ca is placed inside the metal atom oven. The relative fluxes are calculated assuming an ideal solution, such that the vapor pressure of each metal in the oven is equal to its mole fraction times the vapor pressure of the pure metal at the oven temperature of 1000 °K. The resulting chemiluminescence spectrum is resolved into at least one spectral feature associated with each element, and relatively free of overlap as follows: the BaCl C–X $\Delta v = 0$ sequence; the SrCl A–X $\Delta v = +1$ sequence; and the CaCl A–X $\Delta v = 0$ sequence. Previous experiments with pure metals give the ratio of the total visible photon emission to each spectral feature; thus the relative photon emission cross section can be derived. Since the crossed-beam reaction conditions allow most metal atoms to pass through the reaction zone without reaction, the photon emission cross sections must be divided by the reaction cross sections (see Sec. III. E) to give the relative photon yield, the number of photons per reactive encounter. The results are presented in Table III.

It is difficult to ascertain a clear trend in the relative visible photon yields for Ba, Sr, and Ca since the electronically excited products of each reaction produce varying amounts of emission in the infrared. If one compares only the relative photon yield for the MCl C state, it can be see that the yield of the SrCl C state is lower than that of the C states of CaCl or BaCl.

TABLE III. Cross sections and photon yields.

Metal M	Reactive cross section σ (Å^2)	MCl C state relative photon yield Q_c	Total relative photon yield Q
Ba	150	10	a
Sr	130	1.6	1.0
Ca	100	7.2	3.5
Mg	90	...	...

[a]A value for Q is quite uncertain in the case of $Ba + ClO_2$ because of the difficulty in measuring the BaCl A and B state emission.

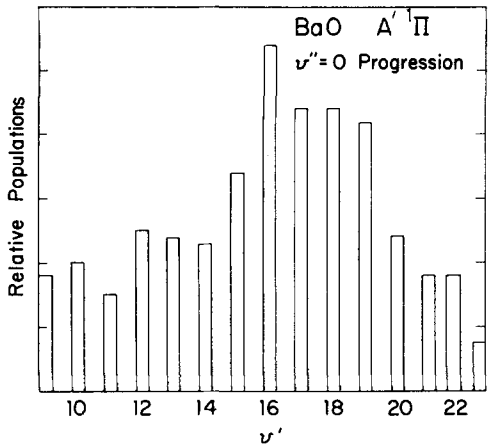

FIG. 7. Relative vibrational populations of the BaO $A'\,^1\Pi$ state formed in the reaction $Ba + ClO_2$. The $v' = 9$–11 populations are less certain because of the detector response.

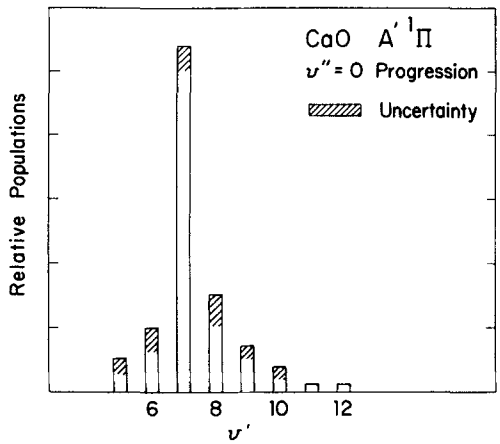

FIG. 9. Relative vibrational population of the CaO $A'\,^1\Pi$ state formed in the reaction $Ca + ClO_2$. The uncertainties are derived by comparing different sequences. The $v' = 5$ and 6 populations are less certain because of detector response.

A separate comparison of $Ba + ClO_2$ with the reaction $Sm + N_2O$ gives a comparable photon yield for both reactions. This implies an absolute photon yield of about 1%.[7]

3. Vibrational

Within the MO A'–X electronic band system, individual vibrational transitions could be assigned and the relative vibrational distribution determined from the intensity of emission from each identified vibrational band of the corrected spectrum. This intensity is obtained either from the area under a band with the estimated contributions of neighboring bands subtracted out, or from the height of the identified bandhead. Given in photon sec^{-1}, the intensities are divided by $q_{v'v''}\nu^3(v', v'')$, the product of the Franck–Condon factor, and the cube of the emission frequency. The Franck–Condon factors are calculated using RKR potentials with Hulbert–Hirschfelder extensions. For the CaO and SrO A' states, the use of the spectroscopic constants ω_e, $\omega_e x_e$, B_e, and α_e of Capelle, Broida, and Field[18] must be restricted to $v' \leq 7$ in order that the inner limb of the RKR potential is well behaved.

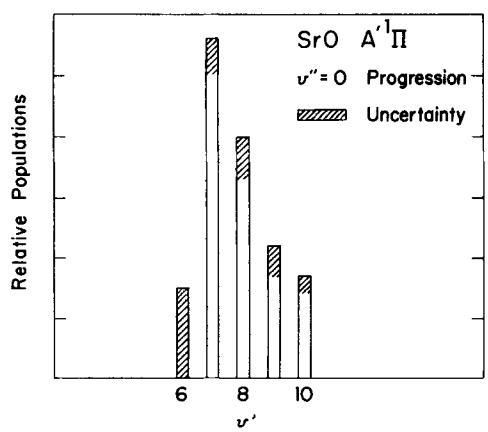

FIG. 8. Relative vibrational populations of the SrO $A'\,^1\Pi$ state formed in the reaction $Sr + ClO_2$. The uncertainties are derived by comparing different sequences. The $v' = 6$ population is less certain because of detector response.

In Figs. 7–9, the BaO, SrO, and CaO vibrational population distributions are shown, using different v' progressions. The close agreement lends credence to the result, namely, the vibrational population distribution in the MO A' state is distinctly non-Boltzmann in character, peaking at $v' = 8$ for CaO, $v' = 6$ for SrO, and $v' \approx 15$–18 for BaO. R. W. Field has suggested to us that the maxima in Figs. 7–9 correspond approximately to the v' levels for which the X state crosses the A' state. Unfortunately, the data for low v' arise from red to infrared transitions that are less accurately measured. Nevertheless, the existence of vibrational population inversions in these electronically excited states seems well established.

4. Rotational

Within a vibrational band, the relative rotational distribution may be found by comparing the area under individual rotational lines. However, a high resolution spectrum of the chemiluminescence is too noisy to justify this procedure. In fact, only for MO* is it possible to even resolve the shapes of the rotational distribution. Instead, a Boltzmann distribution, characterized by a rotational temperature, is assumed, and a least squares fit is made between the calculated chemiluminescence spectrum and the measured spectrum for several vibrational bands, namely, BaO A'–X (17, 0); and CaO A'–X (7, 0), (8, 0), (9, 0), and (10, 0). The best rotational temperatures are between 2300 °K and 2400 °K for all the v' levels studied with no apparent trend going from Ba to Ca or from $v' = 7$ to $v' = 10$. In Ca this corresponds to a most probable J' value of 49 and in Ba to 62.

E. Total cross section

The total reactive cross section or rate constant serves as an important measure of the significance of a reaction process and also as an aid in understanding the reaction mechanism. An approximation to the total reactive cross section may be obtained from a determination of the phenomenological cross section for metal

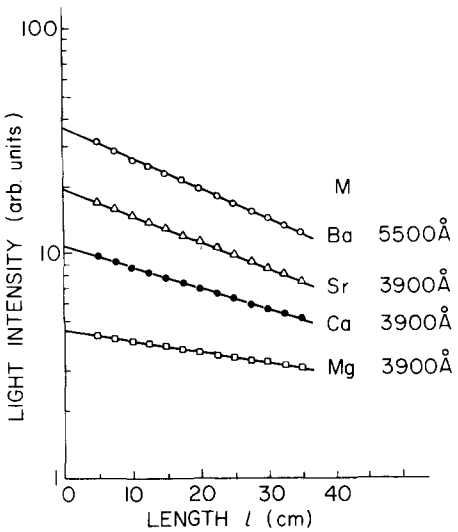

FIG. 10. Plot of the logarithm of the chemiluminescence vs the distance the metal beam travels from the collimating slit to the zone viewed by the photomultiplier. Corning filters are placed in front of the photomultiplier to isolate the wavelength regions indicated.

removal, representing all processes that scatter metal atoms from the beam. For this purpose, we measured the variation of the chemiluminescent intensity as a function of flight distance when a beam of metal atoms travels along the axis of a cylindrical tube filled with ClO_2 gas at a known pressure (see Fig. 1). By analogy to Beer's law for light absorption, we obtain

$$I(l)/I(l=0) = \exp(-\sigma c l) \ , \tag{7}$$

where σ is the phenomenological cross section in cm^2, c is the ClO_2 concentration in molecules per cm^3, l is the path length in cm, and $I(l)/I(l=0)$ is the fraction of chemiluminescent intensity at position l. Equation (7) is based on the previous conclusion (see Sec. III.B) that the chemiluminescence is proportional to the metal atom flux,[34] and is verified by the straight lines observed in the data presented in Fig. 10. The derived cross sections are given in Table III. The relative values should be accurate to within 10%, but the absolute values of these cross sections may be in error by as much as 50% because of the difficulty of determining the ClO_2 pressure in the glass tube while the metal beam is traversing it.

IV. DISCUSSION

The $M + ClO_2$ chemiluminescent reactions where M is an alkaline earth atom have two striking features: (1) the production of MCl* in various electronic states; and (2) the production of MO* in almost exclusively the $A'\,^1\Pi$ rather than the nearly isoenergetic $A\,^1\Sigma^+$ state. We explore here what reasons might be offered for preference of this reaction system for central-atom attack or for end-atom attack leaving the products in a specific excited state.

The alkaline earth atoms have low ionization potentials, which do not greatly exceed those of the alkali atoms. Thus we expect the reactions of the alkaline earth atoms to resemble those of the alkali atoms, characterized by large cross sections and the sudden switch from covalent to ionic interaction. This leads us naturally to apply the rather familiar electron-jump model[35] to the reactions under study. In this model, reaction is initiated by a valence electron of M being transferred to the halogen-containing molecule ClO_2. Subsequent interaction of M^+ with ClO_2^- leads to product formation.

According to a very simplified picture of the electron-jump mechanism, the covalent curve $M + ClO_2$ crosses the ionic curve $M^+ + ClO_2^-$ at a distance r_c given by

$$r_c(\text{Å}) = \frac{14.38}{\text{I. P.(M)} - \text{E. A.}(ClO_2)} \ , \tag{8}$$

where I. P.(M) is the ionization potential (eV) of the metal atom M, and E. A.(ClO_2) is the vertical electron affinity (eV) of the ClO_2 molecule. The ionization potentials for the alkaline earth atoms range from 7.64 eV for Mg to 5.21 eV for Ba. The vertical electron affinity of ClO_2 may be taken as 3.43 eV, its adiabatic value,[36] since only a small change in bond angle is anticipated to occur between ClO_2^- and ClO_2. Thus, in going from $Mg + ClO_2$ to $Ba + ClO_2$, r_c varies from 3.5 Å to 8.2 Å and the cross section, estimated simply as πr_c^2, ranges from 40 $Å^2$ to 210 $Å^2$. While the comparison with the total phenomenological cross sections (90 $Å^2$ for $Mg + ClO_2$ and 150 $Å^2$ for $Ba + ClO_2$) is quantitatively rather poor, the electron-jump model does correctly predict the size and trend of the reactive cross sections.

The subsequent reaction dynamics depend on the manner in which the metal cation M^+ and molecular anion ClO_2^- approach to form the reaction products. From the failure of the various internal state distributions to be characterized by temperatures, it would seem that whatever the nature of this interaction, it must be direct, rather than proceeding through some long-lived collision complex, which would tend to equilibrate the reaction exoergicity among the possible degrees of freedom of the complex. We begin by considering the nature of the ClO_2^- anion.

The bonding and geometry of the AB_2 triatomics were first schematized by Mulliken[37] and by Walsh,[38] who considered the effects of bending on the ordering of the molecular orbital energies. They predicted that BAB triatomic molecules with 16 or fewer valence electrons would be linear, while BAB triatomics with 17 to 20 valence electrons would be bent. Moreover, the BAB bond angle increasingly becomes more acute in going from 17 to 20 valence electrons. More detailed quantum calculations support this model.[39] The chlorine dioxide radical, with 19 valence electrons, proves to be no exception, having an OClO bond angle of 117.5°.[40]

The ground electronic configuration of ClO_2 is $\ldots (3a_1)^2 (2b_1)^1$. The half-occupied $2b_1$ orbital correlates with an antibonding $\bar{\pi}_u$ orbital in the linear triatomic. Figure 11 shows that the $2b_1$ orbital is composed from the superposition of $p\pi$ orbitals on the end O atoms that are out of phase with a $p\pi$ orbital on the central Cl atom. The relative coefficients of the atomic orbitals depend on the ionization potentials of the atoms. Because the

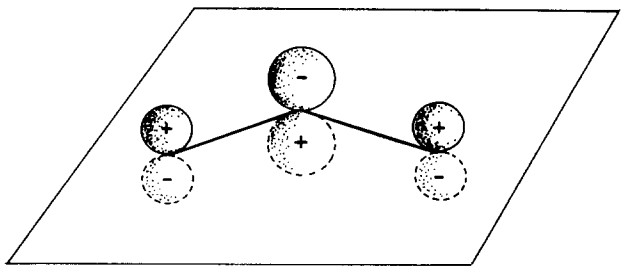

FIG. 11. Schematic drawing of the (half-occupied) antibonding $2b_1$ orbital in ClO_2. This orbital has a node in the plane of the OClO molecule (as shown). The charge distribution is antibonding in character between the central Cl atom and the terminal O atoms, but bonding between the two O atoms.

ionization potential of the O atom is greater than that of the Cl atom, the $1b_1$ orbital has most of its contribution from occupation of the O atomic orbitals while the $2b_1$ orbital has most of its contribution from occupation of the Cl atomic orbital.[41]

Consider the case where the ClO_2^- anion corresponds to the filling of the $2b_1$ molecular orbital. As seen in Fig. 11, this weakens the Cl–O bonds by placing nodes in the charge distribution between Cl and each O atom; this increases the charge density on the central Cl atom. We also note that the $2b_1$ orbital promotes bonding of the two O atoms. The Cl–O bond length[40] in ClO_2 is 1.47 Å, and the two O atoms are separated by about twice the internuclear equilibrium separation in O_2. We picture that an electron jump that fills the $2b_1$ molecular orbital of ClO_2 causes the OClO angle to become more acute, directing the motion of the two O atoms toward one another, since at the same time, the Cl–O bonding is weakened, and attack of the central Cl by the incoming metal cation is facilitated.

The subsequent product distribution then depends in a detailed manner on the interaction in the product exit valley. We imagine that the formation of MCl involves the curve crossings between M^+Cl^- and the various states of MCl. The excited states of MCl are strongly bound Rydberg states, described by an excited nonbonding electron of the metal atom surrounding an MCl^+ core. The MCl bond energy is very large, in fact often larger than its ionization potential.[42] Consequently, some collision trajectories result in the escape of the electron to form ionic products of MCl^+ and either $O_2 + e^-$ or O_2^-, while other trajectories lead to the formation of MCl in various excited electronic states or the ground state. Our photon yields suggest that the ground state product is dominant. Initially we anticipated that the production of excited states should be largest for that pair of collision partners $M^+ + Cl^-$ having the largest curve crossing r_c. Since the total photon yields from MCl* show no consistent trend (see Table III), we must conclude that the nonadiabatic behavior for these reaction systems is not simple.

So far we have concentrated on the attack of the central Cl atom to form MCl*. We now consider the attack of the end O atoms. The $2b_1$ orbital of ClO_2 may cause the ClO_2^- anion to have a double minimum, i.e., unequal Cl–O bond lengths.[43] The possibility that the first excited state of ClO_2 has a double minimum has long been debated.[44,45] This suggests that ClO_2^- may decompose asymmetrically in some trajectories. The possibility of O^- splitout may be enhanced by the electrostatic interaction with M^+. We also note that conservation of orbital symmetry *prevents* the s electron on the metal atom from transferring into the $2b_1$ orbital on ClO_2 if either C_{2v} symmetry is retained or if the metal atom approaches ClO_2 in the plane of the molecule. In these instances, the ClO_2^- anion may once again dissociate into O^- and ClO, since the electron affinity of ClO_2 exceeds the O–ClO bond energy. Thus, the MO product should correlate with $M^+ + O^-$.

The electronic states of the alkaline earth oxides are summarized as follows.[15,46] The MO molecules have eight valence electrons. The ground state of MO has the electronic structure $M^{++}O^{--}$ corresponding to the simple orbital description $(O; 2s\sigma)^2(O; 2p\sigma)^2(O; 2p\pi)^4\ X\,^1\Sigma^+$. The low-lying excited states have the description

$$(M; ns\sigma)^1(O; 2s\sigma)^2(O; 2p\sigma)^1(O; 2p\pi)^4\ A\,^1\Sigma^+ \qquad (9)$$

and

$$(M; ns\sigma)^1(O; 2s\sigma)^2(O; 2p\sigma)^2(O; 2p\pi)^3\ A'\,^1\Pi \quad a\,^3\Pi\ . \qquad (10)$$

The $A\,^1\Sigma^+$ and $A'\,^1\Pi$ states have their minima at approximately the same energy. Hence, at first glance it is difficult to understand why one state should be preferentially populated with respect to the other. However, at large internuclear distances, the $(O; 2p\sigma)$ orbital is more bonding than the $(O; 2p\pi)$ orbital, causing the $A'\,^1\Pi$ state to have a lower energy at larger internuclear separations. Consequently, we speculate that as M^+ and O^- approach each other, the MO $A'\,^1\Pi$ state is preferentially populated, in accord with the experimental observations.

We note that the ground state of the MO molecule does not correlate with the approach of M^+ and O^-. This suggests the possibility that the $M + ClO_2$ reactions, which are specific to the population of one excited state over another, may also be specific to the population of the A' state compared to the X state. If this conjecture is confirmed, it has potentially important consequences for the achievement of electronic population inversions by chemical reaction.

ACKNOWLEDGMENTS

We thank Jeffrey B. Johnson for his assistance in preparing and handling the ClO_2 samples. This work is supported by the U. S. Army Research Office and the U. S. Air Force Office of Scientific Research.

*Deutsche Forschungsgemeinschaft Fellow. Present address: Fakultät für Physik der Universität Bielefeld, D 4800-Bielefeld, West Germany.

†National Science Foundation Energy-Related Fellow.

[1]For a review, see M. F. Golde and B. A. Thrush, Adv. At. Mol. Phys. 11, 361 (1975).

[2]For the first study of atomic chemiluminescence under beam

conditions, see M. C. Moulton and D. R. Herschbach, J. Chem. Phys. 44, 3010 (1966); and for molecular chemiluminescence see Ch. Ottinger and R. N. Zare, Chem. Phys. Lett. 5, 243 (1970).
[3]C. D. Jonah, Ch. Ottinger, and R. N. Zare, J. Chem. Phys. 56, 263 (1972); C. D. Jonah and R. N. Zare, Chem. Phys. Lett. 9, 65 (1971).
[4]J. L. Gole and R. N. Zare, J. Chem. Phys. 57, 5331 (1972).
[5]A. Schultz and R. N. Zare, J. Chem. Phys. 60, 5120 (1974).
[6]R. C. Oldenborg, J. L. Gole, and R. N. Zare, J. Chem. Phys. 60, 4032 (1974).
[7]C. R. Dickson and R. N. Zare, Chem. Phys. 7, 361 (1975).
[8]R. C. Oldenborg, C. R. Dickson, and R. N. Zare, J. Mol. Spectrosc. 58, 283 (1975).
[9]C. R. Dickson, J. B. Kinney, and R. N. Zare, "Determination of D_0^0(BaI) from the chemiluminescent reaction $Ba+I_2$," Chem. Phys. (to be published).
[10]Crossed beams have also been employed by D. M. Manos and J. M. Parson, J. Chem. Phys. 63, 3575 (1975).
[11]F. Engelke and R. N. Zare in *Electronic and Atomic Collisions: Abstracts of Papers of the IXth International Conference on the Physics of Electronic and Atomic Collisions*, edited by John S. Risley and R. Geballe (University of Washing Press, Seattle, 1975), Vol. II, p. 928.
[12]BrCl* emission has been observed in the flow reaction between Br and ClO_2 and attributed to attack of the central Cl atom by Br (M.A.A. Clyne and J. A. Coxon, Chem. Commun. 1966, 285). More recently, M. A. A. Clyne and J. A. Coxon, Proc. R. Soc. London Ser. A 303, 207 (1968) have suggested that the chemiluminescence arises instead from the reaction between Br and the ClOO isomer.
[13]W. Bray, Z. Phys. Chem. 54, 569 (1906); G. Brauer, *Handbook of Preparative Inorganic Chemistry* (Academic, New York, 1963).
[14]W. Kuhn, H. Martin, and K. H. Eldau, Z. Phys. Chem. Abt. B 50, 213 (1941).
[15]R. W. Field, J. Chem. Phys. 60, 2400 (1974).
[16]C. J. Hsu, W. D. Krugh, H. B. Palmer, R. H. Obenauf, and C. F. Aten, J. Mol. Spectrosc. 53, 273 (1974).
[17]J. C. Wyss and H. P. Broida, J. Mol. Spectrosc. 59, 235 (1976).
[18]G. A. Capelle, H. P. Broida, and R. W. Field, J. Chem. Phys. 62, 3131 (1975).
[19]R. W. Field, G. A. Capelle, and C. R. Jones, J. Mol. Spectrosc. 54, 156 (1975).
[20]H. W. Cruse, P. J. Dagdigian, and R. N. Zare, J. Chem. Phys. 60, 2330 (1974).
[21]A. N. Nesmeyanov, *Vapor Pressure of the Elements* (Academic, New York, 1963).
[22]R. N. Zare, Ber. Bunsenges. Phys. Chem. 78, 153 (1974).
[23]W. Finkelnburg and H. J. Schumacher, Z. Phys. Chem. Bodenstein Festband 704 (1931).
[24]I. P. Fisher, Trans. Faraday Soc. 63, 684 (1967).
[25]D. D. Wagman, W. H. Evans, V. B. Parker, I. Halow, S. M. Bailey, and R. H. Schumm, Natl. Bur. Stand. (U.S.) Tech. Note 270-3 (1967).
[26]B. deB. Darwent, Natl. Stand. Ref. Data Ser. Natl. Bur. Stand. 31, 26 (1970).
[27]P. J. Dagdigian, H. W. Cruse, A. Schultz, and R. N. Zare, J. Chem. Phys. 61, 4450 (1974).
[28]C. Batalli-Cosmovici and K. W. Michel, Chem. Phys. Lett. 16, 77 (1972).
[29]A. G. Gaydon, *Dissociation Energies of Diatomic Molecules* (Chapman and Hall, London, 1968), p. 267.
[30]L. Brewer and G. M. Rosenblatt, *Advances in High Temperature Chemistry*, edited by L. Eyring (Academic, New York, 1969), p. 1.
[31]K. Schofield, Chem. Rev. 67, 707 (1967).
[32]R. Colin, P. Goldfinger, and G. Jeunehomme, Trans. Faraday Soc. 60, 306 (1964).
[33]J. Drowart, G. Exsteen, and G. Verhaegen, Trans. Faraday Soc. 60, 1920 (1964).
[34]The contribution from secondary collisions to the observed chemiluminescence is thought to be negligible based on the sharply defined appearance of the glowing beam for nearly the entire length of the tube.
[35]D. R. Herschbach, Adv. Chem. Phys. 10, 319 (1966).
[36]V. I. Vedeneyev, L. V. Gurvich, V. N. Kondratyev, V. A. Medvedev, and Ye. L. Frankevich, *Bond Energies, Ionization Potentials and Electron Affinities*, (Arnold, London, 1966).
[37]R. S. Mulliken, Rev. Mod. Phys. 14, 204 (1942).
[38]A. D. Walsh, J. Chem. Soc. 1953, 2260 and following articles.
[39]R. J. Buenker and S. D. Peyerimhoff, Chem. Rev. 74, 127 (1974).
[40]R. F. Curl, Jr., J. L. Kinsey, J. G. Baker, J. C. Baird, G. R. Bird, R. F. Heidelberg, T. M. Sugden, D. R. Jenkins, and C. N. Kenney, Phys. Rev. 121, 1119 (1961).
[41]R. F. Curl, Jr., J. Chem. Phys. 37, 779 (1962).
[42]K. S. Krasnov, Teplofiz. Vyso. Temp. 3, 927 (1965) [High Temp. (USSR). 3, 865 (1965)].
[43]R. S. Mulliken, Can. J. Chem. 36, 10 (1958).
[44]J. B. Coon, F. A. Cesani, and C. M. Loyd, Discuss. Faraday Soc. 35, 118 (1963).
[45]J. C. D. Brand, R. W. Redding, and A. W. Richardson, J. Mol. Spectrosc. 34, 399 (1970).
[46]J. G. Pruett and R. N. Zare, J. Chem. Phys. 62, 2050 (1975).